Evaluation of Wall Inclination Effect on the Dynamic Response of Mechanically Stabilized Earth Walls Using Shaking Table Tests

Tirtha Sathi Bandyopadhyay, Indian Institute of Technology Patna, India
Sumit Kumar Nandan, Indian Institute of Technology Patna, India
Pradipta Chakrabortty, Indian Institute of Technology Patna, India*
https://orcid.org/0000-0002-8852-2596

ABSTRACT

Shaking table tests were conducted in this study to determine the effect of facing wall inclinations, and the density of the backfill. Reduced-scale models reinforced with two layers of geogrid and fine sand as backfill were studied to identify the dynamic behaviour of mechanically stabilised earth walls. Five different angles of inclination of the facing walls were considered to study its effect on the responses. All seven models were excited by stepped amplitude sinusoidal base accelerations with incrementally increasing peak ground acceleration amplitudes and constant frequencies. The model wall's responses are compared in terms of the acceleration amplification and lateral displacements of the wall measured at different elevations. These tests revealed that horizontal displacement of the wall was maximum at the middle position of the wall. Minimum displacement was observed in the 20° inclined wall towards the backfill soil, which was 35% lower than the vertical wall. The accelerations were amplified along with the wall height. The wall having 10° inward inclination with dense backfill showed the maximum amplification (for high PGA). In the last part, an analytical study was conducted to calculate the acceleration amplifications and compared them with the experimental results. Higher values were observed in the case of the analytical approach as compared to the experimental study.

KEYWORDS

Acceleration Amplification Factor, Geogrids, Mechanically Stabilized Earth Walls, Peak Ground Acceleration, Shaking Table Test

INTRODUCTION

Retaining structures are indispensable parts of all highway constructions. The geosynthetic reinforced soil (GRS) wall, also known as mechanically stabilized earth (MSE) walls has become a popular substitute to the regular concrete retaining walls in many of today's highway and bridge constructions. A mechanically stabilized earth retaining wall is a composite structure consisting of several layers of compacted backfill soil and reinforcements. Reinforcing elements can be geosynthetics, polymeric or steel strips, etc. which are fixed to the wall. The geosynthetic reinforced soil walls have gained a lot of importance worldwide in the last few decades. The growing applications of these walls in resisting

DOI: 10.4018/IJGEE.310052
*Corresponding Author

seismic ground motions have led to widespread research in this field. Studies show that MSE walls can perform satisfactorily during a severe earthquake (Tatsuoka et al., 1996; Tatsuoka et al., 1997; Pamuk et al., 2004). Tatsuoka et al. (1996) observed base sliding and tilting of the wall for some reinforced soil walls subjected to earthquake loading. Pamuk et al. (2004) found that the seismic shakings were the main sources of damage in the reinforced earth walls. Various researches have been carried out, including full-scale studies (Ling et al., 2005; Bathurst et al., 2009; Yang et al., 2009; Koseki, 2012; Yang et al., 2012; Riccio et al., 2014), reduced-scale model (Murata, 1994; Koseki et al., 1998; Chen et al., 2007; El-Emam and Bathurst, 2007; Huang et al., 2011; Wang et al., 2015; Srilatha et al., 2016; Bandyopadhyay et al., 2021; Nandan et al., 2021) and numerical studies (Bathurst and Hatami, 1998; Ling et al., 2010; Abdelouhab et al., 2011; Liu et al., 2014; Zhang et al., 2014). Bathurst et al., (2009) conducted tests on full-scale modular block walls with reinforcements with different stiffness values. The researchers observed that peak wall deformations decreased with the increase in reinforcement stiffness. Koseki (2012) revealed that the geosynthetic-reinforced soil retaining wall performed satisfactorily compared to the unreinforced wall during past large earthquakes. Koseki et al. (1998) performed shaking table tests and observed that the wall's failure mode was overturning with tilting of the wall face. El-Emam and Bathurst (2007) studied the influence of reinforcement parameters on a small-scale reinforced wall. The researchers concluded that the total facing displacement under base excitation decreased with increased reinforcement length and greater reinforcement layers. Srilatha et al.(2016) conducted shaking table tests by changing the base shaking frequency to study the dynamic behaviour of unreinforced and reinforced soil slopes with clayey sand as backfill. The researchers concluded that reinforced models showed lesser displacement compared to unreinforced in all frequencies. Bathurst and Hatami (1998) conducted numerical investigations to check the effect of reinforcement stiffness, reinforcement length and base boundary conditions on the seismic response of MSE walls using the finite difference method. Researchers reported that wall displacements and reinforcement loads accumulated during base shaking. The wall displacement diminished with higher reinforcement stiffness and greater length of the reinforcement. Most of these studies carried out the seismic analysis of the MSE walls by varying different parameters and found MSE walls as stable and effective structures under dynamic loadings. However, most of these researches have not studied the effect of inclination of facing wall and the backfill parameter's effects on dynamic responses.

The quality of compaction of the backfill soil is one of the governing factors in the retaining wall's performance. Lee et al. (1973) investigated the behaviour of small-scale reinforced retaining walls at two different densities of backfill sand. The researchers observed a little difference in failure heights for the loose backfill compared to dense sand backfill. Sakaguchi (1996) found that the proper relative density of soil increases the sand-geosynthetic interaction. Latha and Krishna (2008) studied the effects of backfill relative density on GRS wall's dynamic response using shaking table tests. The researchers used varying relative densities in the range of 37-87%. Lateral deformations of the wall decreased with the increase in the relative densities. Lemnitzer et al. (2012) evaluated the effect of compaction of the backfill sand with relative densities ranging from 40 to 60% for one specimen and 90 to 100% for others. The researchers observed a significant difference of approximately 50% in initial stiffness and ultimate capacity in the passive load-displacement relationship. Latha and Santhanakumar (2015) studied the effect of backfill density on unreinforced and reinforced retaining wall performance. The researchers conducted shaking table tests at 47% and 65% relative densities and observed that the wall's displacement increased with the elevation. Improving the relative density of the backfill resulted in a reduction in wall deformations. Also, accelerations were amplified with the elevation, and it was more at the top of the wall. The above-discussed studies presented the effects of the backfill parameters on the dynamic response of the GRS walls. However, the interaction effect between wall elements and backfill soil density has not been studied.

Facing wall elements provide the required stiffness and could reduce the reinforcement loads. The facing design parameters, including type, size, and orientation, play a vital role in resisting seismic loading. Tatsuoka (1993) reported that in geosynthetic reinforced soil walls with vertical facing, rigid facing is an essential way to obtain stability of the structure. Many researchers have studied the seismic performance of vertical and inclined retaining walls with different types of facings (Bathurst, 2002; Huang and Wang, 2005). Matsuo et al. (1998) performed several model tests with varying facing types (i.e., discrete and continuous) and changing the wall sloping. The researchers concluded that continuous facing had more deformation than a discrete one. Allen and Bathurst (2002) studied twenty numbers of geosynthetic walls with several model configurations. It has been concluded that stiff facing reduced the loads on reinforcement as compared to the flexible one. El-Emam and Bathurst (2005) studied the wall contribution to the MSE wall model's seismic response by changing the wall's inclination. The researchers tested vertical and 10° inward inclined wall's performance and observed that the lateral displacement was high for the vertical wall. The vertical toe load was found to be less for inclined wall models. Jackson et al. (2012) presented an experimental study on reduced-scale rigid faced GRS model walls. The wall inclination was varied from 90° to 70° to the horizontal. Failure of the model was predominantly by overturning with a decrease in wall displacement with a decrease in wall inclination with the vertical.

Based on the available literature, it can be observed that a significant amount of research has been carried out on the effect of backfill density and facing parameters. Studies have shown that inclined walls have performed better in many aspects, such as displacement of wall, and toe loads. However, there are limited studies on the effect of the inclination of the wall in the seismic analysis of MSE walls. No study has been tried to propose an analytical model for estimating dynamic responses in MSE walls. Therefore, the present study has been designed to evaluate the MSE wall model's quantitative response to base shaking with different wall inclinations. A series of shaking table tests were carried out on geogrid reinforced small-scale MSE wall models by changing wall inclinations at two different backfill relative densities. A simple linear analytical model has been formulated to estimate the dynamic response of MSE walls. The results discussed in this study will provide insightful information and design implications for the safe seismic design of MSE walls.

SHAKING TABLE TEST

The shaking table used in this study is designed for applying horizontal one-dimensional (1-D) sinusoidal shaking. The dimensions of the table are 1000 mm long and 700 mm wide. Different combinations of the pulley and the actuator with the belt were used to induce base accelerations with different PGA values. Figure 1 shows the model box mounted on the shaking table. Several researchers have documented

Figure 1. Seismic box mounted on the shaking table

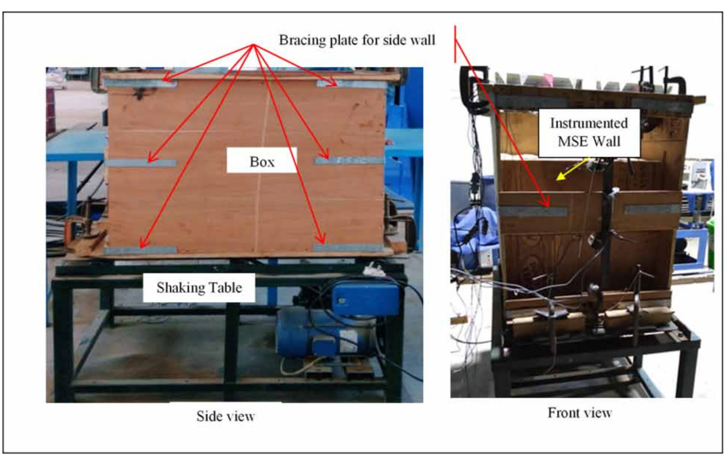

small-scale shaking table tests without considering the scale effects (Koseki et al. 1998; Matsuo et al. 1998). The major problem associated with laboratory model studies is the scaling and boundary effects. The seismic response of the model walls may not truly reflect that of the prototype due to the stress-dependent behaviour of the soil. Hence, the results from this study can be used for understanding the effect of various dynamic shaking parameters on a reinforced slope. Two rigid plywood panels have been used to model the MSE walls. The backfills have been poured at desired density inside a rigid box neglecting the boundary's effect, which could be one of this study's limitations.

MODEL CONFIGURATION AND CONSTRUCTION

GENERAL

Seven models were designed to evaluate the influence of the wall slope and backfill density on the dynamic response of MSE walls. Table 1 shows the detailed wall configurations and relative densities of the backfill for the models. The MSE wall model consists of soil deposits in a 655 mm long, 580 mm wide wooden box with bracing systems opened from the front and mounted on the shaking table. Considering a scaling factor of 10, as suggested by Iai (1989), the model walls may resemble a prototype of a height of 5400 mm or 5.4 m. The design backfill relative densities were selected at about 40% and 70%. For creating the soil deposit at pre-decided relative densities, the sand was rained from certain heights into the box. The soil was filled in lifts of four layers. The relative densities of each layer of the lifts and the average densities are reported in Table 1. The achieved relative densities measured after the sand raining was varied between 42 to 44% for loose sand and 70% for dense sand backfill.

Table 1. Test model configuration

Test model	Backfill property	Layer wise relative density (%)	Average Relative Density (%)	Wall inclination (θ)
L_0Ver	Loose	Layer 1- 42.9 Layer 2- 44.1 Layer 3- 43.8 Layer 4- 43.5	43.6	Vertical
D_0Ver	Dense	Layer 1- 70.3 Layer 2- 69.9 Layer 3- 70.1 Layer 4- 69.8	70.0	Vertical
L_10Out	Loose	Layer 1- 42.5 Layer 2- 41.5 Layer 3- 41.1 Layer 4- 42.1	41.8	10^0 outwards
L_5In	Loose	Layer 1- 42.6 Layer 2- 41.2 Layer 3- 41.9 Layer 4- 42.8	42.1	5^0 inwards
L_10In	Loose	Layer 1- 42.2 Layer 2- 41.1 Layer 3- 42.7 Layer 4- 42.9	42.5	10^0 inwards
D_10In	Dense	Layer 1- 70.1 Layer 2- 69.5 Layer 3- 70.7 Layer 4- 69.8	70.0	10^0 inwards
L_20In	Loose	Layer 1- 42.5 Layer 2- 41.7 Layer 3- 42.2 Layer 4- 42.1	42.1	20^0 inwards

The Federal Highway Administration (Elias et al., 2001) guidelines suggest that the length of reinforcement for MSE walls should not be less than *0.7H'*, where *H'* is the height of the wall. In this study, the height of the wall was 540 mm on the model scale. Therefore, the length of the reinforcement was kept as 400 mm which is greater than *0.7H'*. A spacing of 270 mm between the two layers of the geogrid was calculated considering both the internal and external stability of the wall. According to FHWA guidelines, all models were found to be safe in static loading conditions for the considered length and spacing of the reinforcement. Three stepped increased horizontal sinusoidal motions of 10 seconds duration each were applied by changing the frequency of the shaking table motor (frequency range of motor is 1.41 Hz to 4.46 Hz which can induce a PGA of 0.1g to 1g). Figure 2 shows the schematic diagrams of all the instrumented reinforced wall models.

Figure 2. Schematic layout of MSE wall models (all dimensions are in mm) and instrumentation: model with (a) Vertical facing, (b) Inward inclined facing, (c) Outward inclined facing

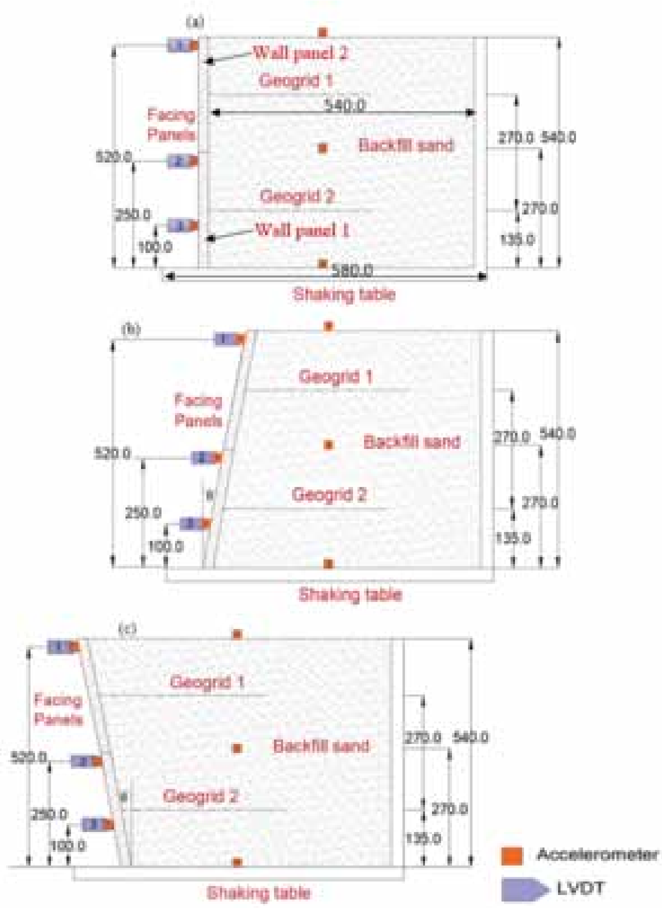

MATERIALS USED IN MSE WALLS

Backfill Sand

Good quality granular soils are preferred as backfill materials for the construction of geosynthetic reinforced walls. But due to the unavailability of these soils, locally available soil is sometimes used as backfill. Locally available sand has been used in this study. Sieve analysis result of the used soil sample classified the soil as poorly graded sand (SP) as per the Unified Soil Classification System (USCS). The grain size distribution curve is shown in Figure 3.

Figure 3. Grain size distribution curve for backfill sand

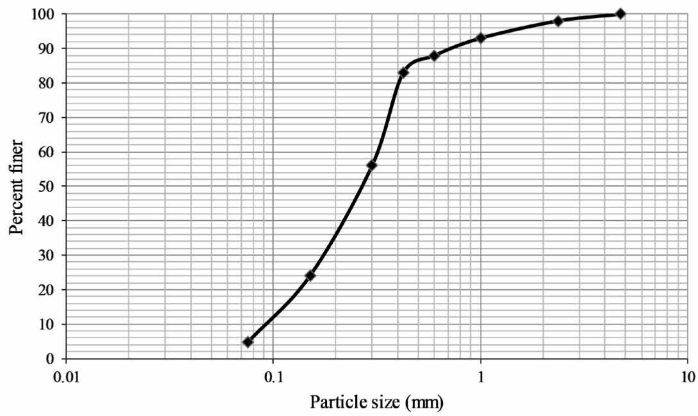

The specific gravity of the sand was estimated as 2.69. The sand's dynamic properties were calculated using strain-controlled consolidated undrained cyclic triaxial tests as per ASTM guidelines (ASTM D3999/ D3999M−11). The value of the modulus of elasticity was calculated using the load and displacement curve. Further, the shear modulus was calculated using the relationship between the modulus of elasticity and Poisson's ratio. Shear wave velocity was then obtained using shear modulus relation with the density of sand. The physical and dynamic properties of sand are tabulated in Tables 2 and 3, respectively.

Table 2. Physical properties of the backfill sand used in MSE walls

Parameters	Values
Uniformity coefficient (C_u)	3.44
Coefficient of curvature (C_c)	1.137
Minimum density (g/cm^3)	1.434
Maximum void ratio (e_{max})	0.876
Maximum density (g/cm^3)	1.708
Minimum void ratio (e_{min})	0.575

Table 3. Dynamic properties of backfill soil

Backfill soil relative density (Rd) in %	Shear modulus (G) in MPa	Damping ratio (ξ) in %	Shear wave velocity (V_s) in m/s
42	15.5	18.48	103.50
70	25.0	14.77	125.63

REINFORCEMENT

Biaxial geogrids have excellent tensile modulus in both longitudinal and transverse directions, aperture stability and high strength at low strain led to better performance than uniaxial geogrids. Latha and Somwanshi (2009) found that the bearing capacity improvement was lesser in uniaxial than biaxial geogrid. Several researchers have used biaxial geogrids to study the seismic performances of reduced-scale MSE walls (Latha and Santhanakumar, 2015; Srilatha et al., 2016). In this study, two layers of biaxial geogrids with square aperture have been used as reinforcing material. The aperture size was 35 mm × 35 mm with a thickness of 1.6 mm, made up of firm polyester coated with the bituminous solvent, which provides high frictional characteristics and grabbing power. The length of the geogrids was kept 400 mm. The tensile strength and shear modulus of the geogrid used in the study was 13 MPa and 117 MPa, respectively. Matsuo et al. (1998) studied the reinforcement effect on the dynamic response of model walls without considering the scale effect of the geosynthetics. Scale effect of the geogrid specimen was also not considered in this study.

Facing Wall

The wall is relatively thin, with the primary function of preventing erosion of the structural backfill. The walls were constructed with different wall inclinations. The facing panel was made using two rectangular wooden plates with 580 mm (wide) × 270 mm (tall) with a modulus of elasticity of 8305 MPa. The thickness of the facing panels was 25 mm. The top plate was placed directly on the bottom very cautiously. They got to hold at their sides, and due to friction provided from the sidewalls, stability of the facing walls was achieved. Four hook nails have been attached to each facing panel to provide the connection to geogrid. The toe restraint condition of the model facing panel was hinged type (i.e., restrained in the vertical direction only and free to rotate).

DATA ACQUISITION SYSTEM AND INSTRUMENTATIONS

The models were instrumented with accelerometers and LVDTs to measure the dynamic response of the MSE walls. Three LVDTs having measurement accuracy up to 0.01 mm, were placed at the bottom, middle, and top parts of the facing panel to measure the lateral wall displacements. Accelerometers were placed at facing as well as at the soil backfill to measure acceleration response. For acquiring data from the accelerometers, Bruel and Kjaer set-up was used with *PULSE Labshop,* and for data processing and filtering, *PULSE Reflex* software was used. The schematic layout of MSE wall models and the positions of all the LVDTs and the accelerometers are shown in Figure 2.

BASE INPUT ACCELERATION

Horizontal accelerations were applied to each model in stages with increasing acceleration amplitude. Sinusoidal base input motions with three different peak ground accelerations (PGA), i.e., low-PGA (0.059g), mid-PGA (0.185g), and high-PGA (0.488g) varying from low to high were applied to the MSE wall model using the shaking table. These medium and high-PGA base input motions are very close to the ones reported by Collin et al. (1992). The researchers studied a reinforced retaining wall designed for 0.2g sustained the earthquake motions up to 0.41g. The present study used the low-PGA value to find any effect of the lower PGA input motions on the wall's dynamic response. The recorded base input acceleration time histories are shown in Figure 4 after filtering. The input acceleration time histories with various PGA levels have been shown hereafter removing noise using a bandpass filter of 0.1 Hz to 50 Hz.

Figure 4. Filtered input acceleration time histories with various PGA levels (records are filtered with a bandpass filter of 0.1 and 50 Hz frequencies)

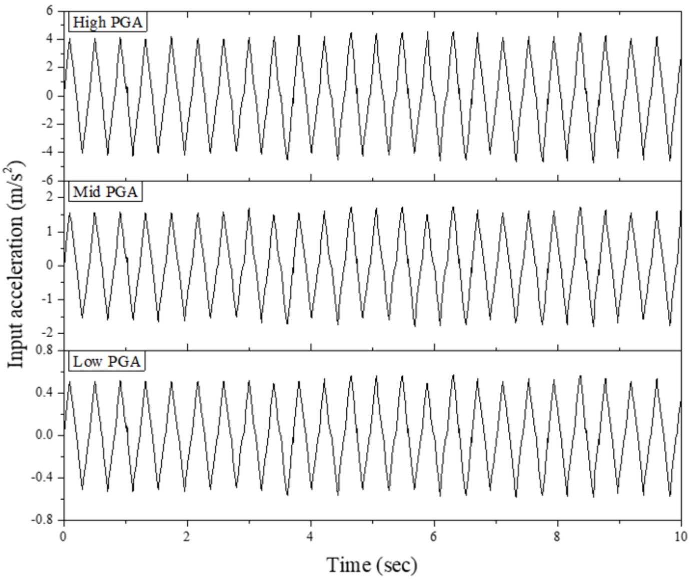

TEST RESULTS

The test results discussed in this section include displacement and acceleration responses of the wall and backfill soil. The acceleration responses obtained from experimental results were compared with the analytical approach. The difference in the values between both the analysis has been shown through graphical representation.

HORIZONTAL WALL DISPLACEMENTS

Effect of Inclination of Facing Panel

The effect of facing wall inclination on the performance of geogrid reinforced wall models is presented here**.** The responses of MSE wall models were compared in terms of horizontal displacements of the wall measured at different elevations. Maximum horizontal displacement responses for five different angles of inclination, i.e., 10° outward, vertical (0°), 5° inward, 10° inward and 20° inward were compared for the loose state of backfill. For the same input motion, the inwardly inclined wall showed less displacement as compared to the vertical wall. Similar observations were reported by El-Emam and Bathurst (2005). The outward inclined wall showed the highest displacement due to the unstable structural configuration. The maximum displacement was measured in the middle of the wall for all cases, as shown in Figure 5.

It may be due to the absence of any connections between the panels in the middle of the wall. The joint between the two facing panels was unable to resist the load on the wall. Hence, greater wall displacement was observed in the middle of the wall. The bottom of the wall experienced a lesser lateral displacement. For better understanding, the wall's height has been represented in the form of the wall's normalized height. It has been calculated as the ratio between the height from the bottom to the total wall height. In high PGA input motion, the 10^0 inclined wall towards the backfill had 7.72%

Figure 5. Effect of wall inclination on horizontal displacement response of the wall in loose backfill sand at (a) Low-PGA, (b) Mid-PGA and (c) High-PGA

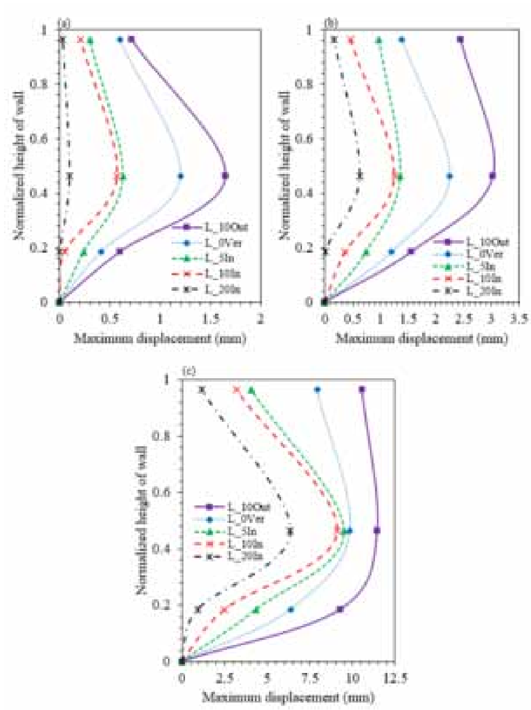

less displacement, and the 20^0 inclined wall model had over 35% less displacement than the vertical wall. It could be because of the decrease in lateral earth pressure with the increase in wall inclination towards the backfill as predicted in pseudo-static earth pressure theory (El-Emam and Bathurst, 2005). The maximum displacement at the middle of the 20^0 inclined wall was 6.35 mm, which resembles the maximum displacement of 63.5 mm in the prototype wall as per the scaling law (Iai 1989). In contrast, the 10^0 outward inclined wall model showed 16% more horizontal displacement than the vertical wall when other criteria remained the same. The MSE wall inclined outward generates active pressure that may not be found in the vertical and inward walls. Due to this reason, an outward wall displaces more compared to other orientations. Displacements of the wall were also checked for an intermediate inclination, i.e., 5^0 inward inclinations, and the values of displacements were observed to be in between vertical and 10^0 inclinations. Similar trends were observed for the low and medium PGA input motions. The outward inclined facing panel showed larger displacements than the vertical wall for low and medium PGA. However, the 20° inward inclined wall showed the least displacement for low and medium input motions.

Effect of Backfill Soil Relative Density

The MSE wall models were also studied to identify the effect of the relative density change of the backfill soil on the wall's displacement behaviour. Two states of the soil backfill's relative density were tested for the three input motions for vertical wall and 10° inward inclined wall. Figure 6 shows the maximum horizontal displacement response of the facing panel varying with the elevation for the soil's two density conditions.

It was observed that with the increase in density, the maximum horizontal displacement decreased. For all the cases, the wall's middle position witnessed the maximum deflection for all three input motions. Comparing all the four models, the vertical wall and loose backfill showed maximum

Figure 6. Effect of change in the backfill soil density on horizontal displacement response of the wall for wall inclination of 0° and 10º inwards at (a) Low-PGA, (b) Mid-PGA and (c) High-PGA

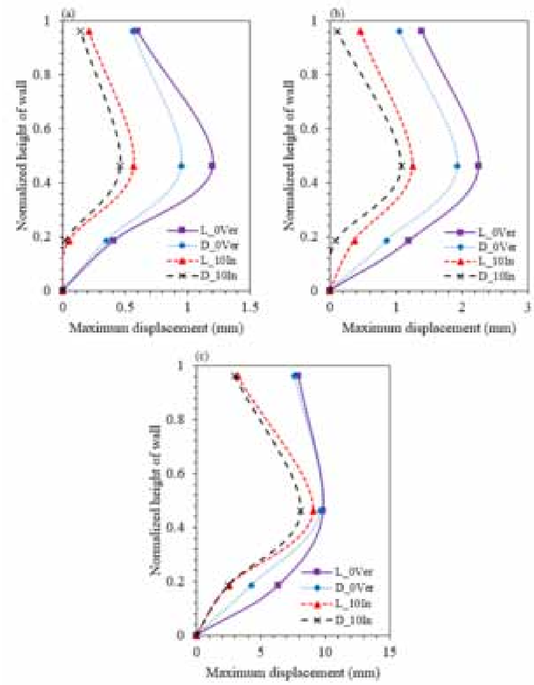

horizontal displacement. The maximum horizontal displacement was reduced by over 3% for a vertical wall with dense backfill for high PGA. Similar observations were found for low and medium PGA values. For medium PGA, maximum displacement at the middle wall was reduced by 14.8%. For low PGA, maximum displacement was reduced by 20.8% in the dense state compared to the loose state. A similar observation was reported by Latha and Santhanakumar (2015). The researchers found that maximum wall deformation was reduced by 18.4% for an increase in the backfill density from 47% to 65% for the rigid wall model. The MSE wall model with a 10° inward inclined wall with dense backfill showed the minimum horizontal displacement for all the input motions at all the wall locations. As compared to the 10° inward inclined wall with loose backfill, the maximum horizontal displacement of the wall with the same inclination in dense backfill was 21.5% less for high PGA. The analysis found that the inwardly inclined walls in the dense state of backfill had better results in terms of wall displacement. It may be due to the combined effect of the inclination and the density of the backfill. The active earth pressure generated in the inwardly inclined wall is less than other conditions, and the higher density soil provides a lesser coefficient of earth pressure. Thus, the inward wall at higher density backfill was found to have the least wall displacements.

ACCELERATION RESPONSE

Acceleration responses were recorded using the accelerometers placed at different locations of the model. Figure 7 shows the acceleration recorded at different locations of the backfill (bottom, middle and top of the backfill) for 10° inward inclined wall with dense backfill for high input motion.

It was observed that the acceleration was amplified by 1.47 and 1.70 times that of the applied input motion at the middle and top of the backfill, respectively. The extent of acceleration amplification of the wall and backfill has been presented in the form of acceleration amplification factor (AAF). The

Figure 7. Acceleration time histories (applied and recorded) at various locations for 10° inward inclined wall with dense backfill (records are filtered with a bandpass filter of 0.1 and 50 Hz frequencies)

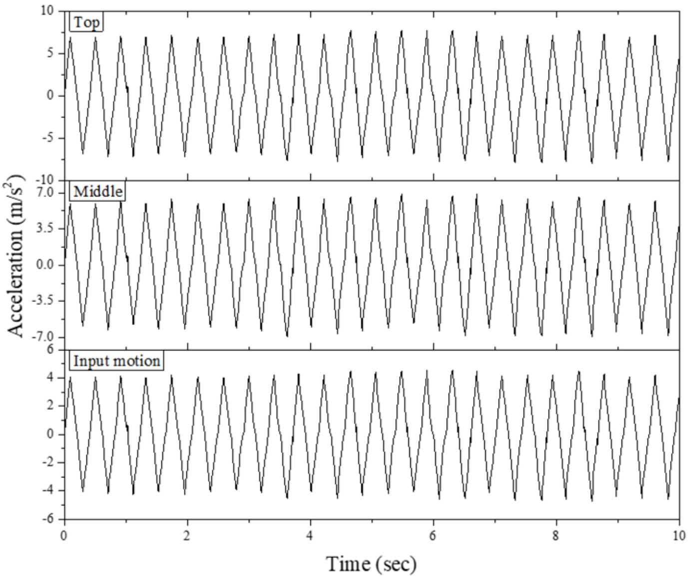

AAF is defined as the ratio of maximum acceleration value obtained at any point to the applied peak acceleration value. The acceleration was found to amplify with the height of the wall and backfill. Figure 8 shows the variation of the amplification factor with the height of the backfill as normalized height.

Figure 8. Acceleration response along with the height of the backfill soil (a) Low-PGA, (b) Mid-PGA, and (c) High-PGA

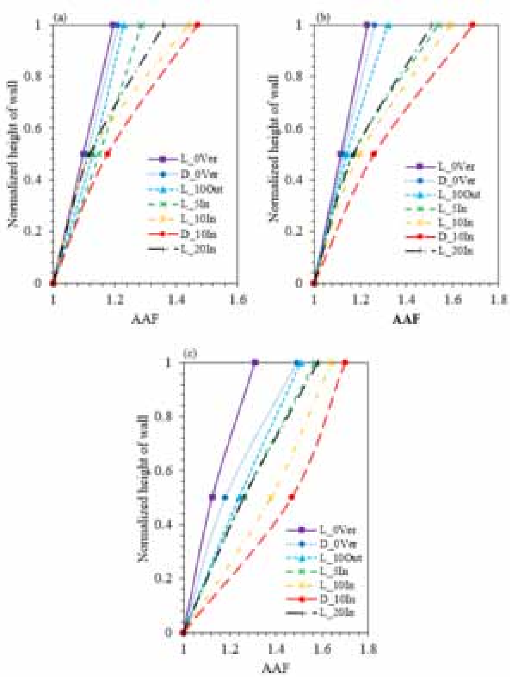

Nonlinear variation was observed for all the models. The acceleration response depends on the properties of the backfill and the wall. The pseudo-static design guidelines assume uniform acceleration over the soil's height in a geosynthetic reinforced soil wall. But several studies have revealed that input acceleration amplifies over the height of the wall and backfill (Latha and Santhanakumar, 2015; Matsuo et al., 1998). The result of the present study also confirms the same observation. Yang et al. (2013) revealed that the AAF is greater than one for a base acceleration lower than 0.4g. The present study revealed that the AAF had been found greater than one for all studied input motions. It can be observed from the results presented in Figure 8 that with the increase in the density, the amplification increased. Dense soil exhibits lesser damping causing higher amplification. It may be the reason for greater AAF in the dense state than the loose sand backfills. The vertical soil experienced 9% and 5% greater AAF in the dense state of soil at the top and middle of the backfill, respectively compared to the loose state at high PGA input motion. The 10° inward inclined wall experienced 4% and 7% higher AAF in dense state at the top and middle of the backfill, respectively. Acceleration response was also compared for the different inclinations of the wall. It was observed that vertical walls in a loose state experienced the least amplification of acceleration. The 10° inward wall in the dense state showed the maximum amplification to be almost 30% higher than the vertical wall at the top under high PGA. The 10° inward and outward walls were observed to have 25% and 16% higher AAF than the vertical in loose state at high PGA. The 5° inward wall had also undergone a similar response as the 10° inward wall. A similar manner of variations was found for the low as well as medium intensity ground motions. It is a well-known fact that damping increases with the reduction in confining pressure (Collin et al., 1992; Bathurst and Hatami, 1998). Thus, the increase in pressure reduces the damping and hence, increases acceleration amplification. But sudden fall of acceleration amplification was observed at 20° inward wall.

Acceleration amplification was also noticed at the facing wall. The acceleration amplification was found to be intensified over the top half of the facing wall. Figure 9 shows the amplification factor's variation with the wall's height as its normalized height.

Figure 9. Acceleration response along with the height of the facing panel (a) Low-PGA, (b) Mid-PGA, and (c) High-PGA

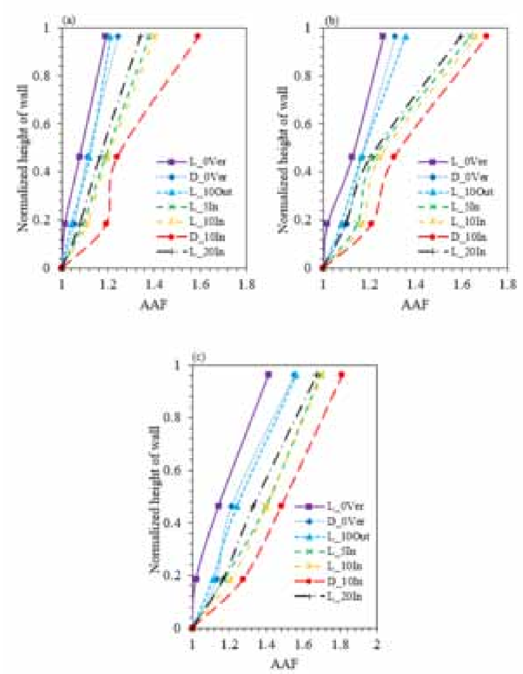

It was observed that the variation of the AAF shows an increasing trend with elevation in a non-linearity manner for all the test models. A similar type of higher velocity generated at the wall's crest was also observed by El-Emam and Bathurst (2005). After comparing the AAF for all the seven models, it was observed that for the same density condition of the backfill, the vertical wall showed the least amplifications. The 10° inward inclined wall in the dense state showed the maximum amplification to be almost 28% higher than the vertical wall at the top for high PGA. The 10^0 outwardly inclined wall model showed intermediate values. 20° inward wall showed lesser amplification compared to 10° and 5° inclined walls. Studies from Jackson et al. (2012) revealed an increase in the wall inclination from vertical increased acceleration. The present study also confirms this observation. It was also noticed that the 20° inward wall experienced less acceleration than the 10° inward inclined MSE wall. A similar type of response was noticed in low and medium PGA input motions.

The change in the backfill density also witnessed significant acceleration amplification along with the height of the wall. The AAF increased by over 3%, 4% and 10% in the dense state compared to the loose state at the top of the wall in the vertical MSE model for high, medium and low PGA values, respectively. For the 10° inwardly inclined wall, the AAF increased by over 5%, 3% and 14% for the dense state compared to the loose state of backfill at the top of the wall for high, medium and low PGA, respectively. The results show that a higher acceleration amplification rate was observed for higher input motions. It could be due to the waves generated from strong input motion repeatedly reflected in the deposit and wall material. This ultimately increases the recorded acceleration level.

A SIMPLE ANALYTICAL STUDY

A simple analytical approach has been adopted in this sub-section to determine the acceleration amplification at different elevations of the backfill soil. The 1-D linear ground response analysis is one of the simple analytical methods to estimate seismic ground amplification. This analytical procedure has been used in this study to estimate acceleration amplification. One-dimensional ground response analysis has been carried out based on the assumption that all boundaries are horizontal in the model and SH-waves propagating in the vertical direction dominate soil response (Kramer, 1996). Hence, the comparison was done for vertical walls only. The effect of MSE wall inclination was not considered in the analytical model. The analytical results obtained for both loose and dense soil backfill with the vertical wall (Models 1 and 2) have been compared with the experimental values. The effects of geogrid layers have also been taken into consideration in the analytical ground response study. The models have been divided into five layers, i.e., three layers of soil and two geogrid layers in the analysis. Figure 10a shows all the layers of soil and geogrid with their dimensions and other properties. Three layers of sand with thicknesses h_1, h_3 and h_5 with their shear modulus and damping ratio values G_1, G_3, G_5, ξ_1, ξ_3, and ξ_5, respectively are shown in Figure 10a. Two layers of geogrid with a thickness of h_2 and h_4 with their shear modulus and damping ratio values G_2, G_4, ξ_2, and ξ_4, respectively are also shown. Figure 10b shows the nomenclature for all the layered soil deposits on a rigid surface, where u_i is the horizontal displacement of the i^{th} layer and z_i is the depth in that layer in the local coordinate system. The rigid base acts as a fixed end. Downward traveling waves in the soil get completely reflected toward the ground surface by the rigid layer, thereby trapping all of the elastic wave energy within the soil. Considering the first layer *(L_1)* as uniform damped soil on the rigid base of the shaking table, from the ground response analysis, the amplification function can be expressed as:

$$F(\omega) = \frac{1}{\sqrt{\cos\left(\frac{\omega h1}{vs1}\right)^2 + \left[\xi 1\left(\frac{\omega h1}{vs1}\right)\right]^2}} \qquad [1]$$

where, ω is the circular frequency and vs_1 is the shear wave velocity.

The L_2 is the layer of geogrid of thickness h_2. Considering L_2 (geogrid) and L_3 (sand layer) lying on elastic soil (L_1), horizontal displacement within a given layer is given by:

$$u_2 (h_2, t) = (A_2 \times e^{ik_2^* h_2} + B_2 \times e^{-ik_2^* h_2}) \times e^{i\omega t} \qquad [2]$$

where, A_2 and B_2 are amplitudes of upward and downward waves in layer L_2 and k_2^* is complex wave number. Expression for displacement in layer L_3 can be written similarly to the parameters for L_3. The shear stress is given as:

$$\tau_2 (h_2, t) = ik_2^* G_2^* \times (A_2 \times e^{ik_2^* h_2} - B_2 \times e^{-ik_2^* h_2}) \times e^{i\omega t} \qquad [3]$$

Using compatibity of displacement and shear stress at the boundaries and introducing α^*, which is the complex impedance ratio, the wave amplitudes for layer L_3 can be obtained from amplitudes of layer L_2 in following manner:

$$A_3 = \frac{1}{2} \times A_2(1+ \alpha_2^*)e^{ik_2^* h_2} + \frac{1}{2} \times B_2(1- \alpha_2^*)\, e^{-ik_2^* h_2} \qquad [4]$$

$$B_3 = \frac{1}{2} \times A_2(1- \alpha_2^*)e^{ik_2^* h_2} + \frac{1}{2} \times B_2(1+ \alpha_2^*)\, e^{-ik_2^* h_2} \qquad [5]$$

A_3 and B_3 being the amplitudes of waves in layer L_3. Transfer function related to displacement amplitudes at L_3 to L_2 is given as:

$$F_{32}(\omega) = \frac{|u3|}{|u2|} = \frac{a3(\omega) + b3(\omega)}{a2(\omega) + b2(\omega)} \qquad [6]$$

Similarly, analysis can be done for layers L_3, L_4 and L_5.

In general, the transfer function relating the displacement amplitude at layer *i* to that at layer *j* is given by:

$$F_{ij} = \frac{|ui|}{|uj|} = \frac{ai(\omega) + bi(\omega)}{aj(\omega) + bj(\omega)} \qquad [7]$$

Because $\left|\ddot{u}\right| = \omega^2 \left|u\right|$ for a harmonic motion, equation 7 also can be used to describe the amplification of accelerations. The above equations were formulated based on the method documented in the literature (Kramer, 1996). Kramer (1996) documented that the transfer function allows easy computation of the response to any complicated loading including earthquake motions. It filters the input signal and produces an output signal. Figure 10c shows a step-by-step procedure for calculating output response from an input acceleration time history. The input motion has been converted into the frequency domain. Next, the location-specific transfer function has been calculated using equation

7 for various depths. The transfer function has been multiplied with the input acceleration Fourier spectrum to obtain the corresponding output acceleration Fourier spectrum. The resultant output acceleration Fourier spectrum has been converted into the time domain to obtain acceleration time history at a specific location. The comparison between experimental and analytical acceleration time histories at mid-depth and top of the backfill soil has also been shown in Figure 10c.

Figure 10. (a) MSE walls model of sand and geogrid layers lying on rigid shaking table (red line showing the plane along which analytical 1-D ground response analyses have been performed); (b) Nomenclature used in the analytical model for layered soil deposits on a rigid surface; (c) Comparison of experimental and analytical acceleration response at mid-depth and top of the backfill (shows top to bottom: experimentally measured and analytically computed acceleration time history, transfer function, Fourier spectra of input, and input acceleration time history)

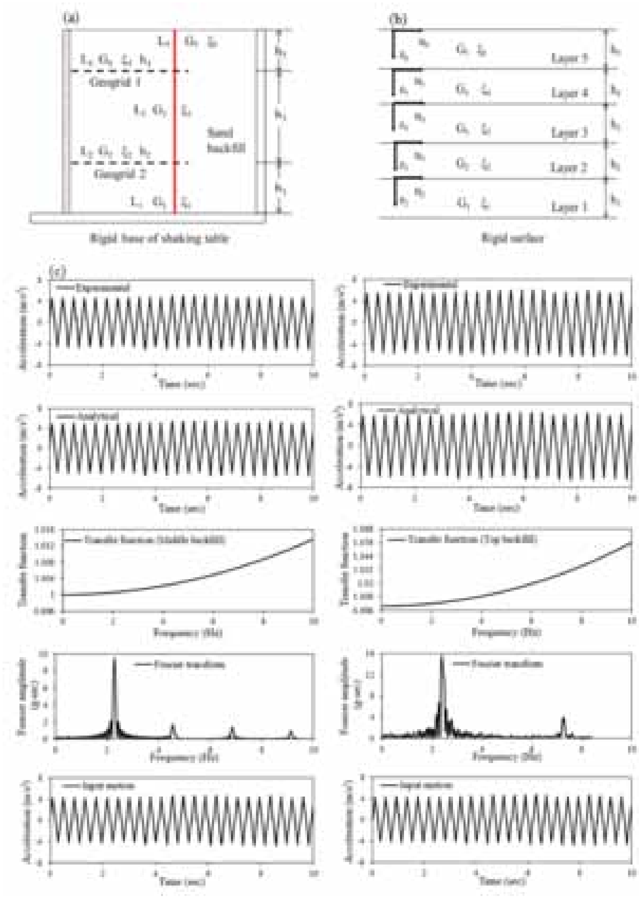

Equation 7 was used to calculate the maximum ground amplifications at the middle (*H/2* depth), *H/4* depth and top of the sand backfill. Figure 11 shows the comparison of the analytical and experimental results in terms of AAF.

The results were compared for both the loose and dense state of the backfill for the vertical wall. From the analysis, it was found that the analytical results showed higher amplification as compared to the experimental results. The analytical values do not consider soil-reinforcement interaction, due to which higher AAF was obtained. However, the pattern was found to be similar for both loose and dense soil backfill. There was nearly 4% variation between analytical and experimental results in

Figure 11. AAF comparison between experimental and analytical results AAF comparison between experimental and analytical results

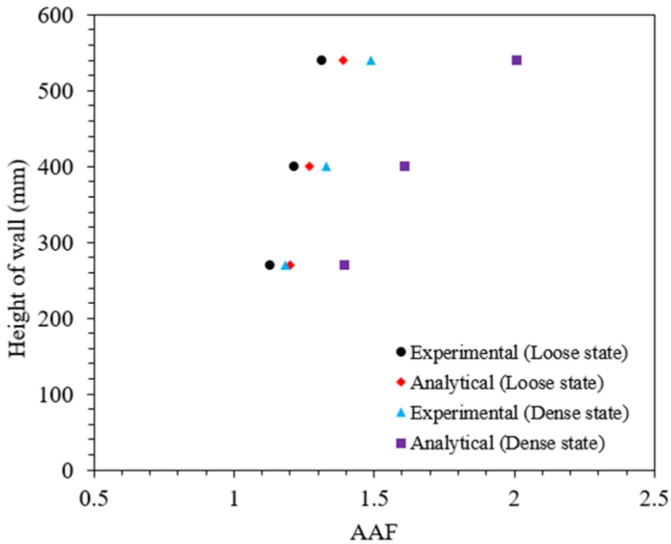

the amplification at the three-fourth height of the loose sand backfill. In contrast, about 6% variation was observed at the top of the backfill for the same density. At the middle height of the backfill, the analytical study's amplification factor was about 7% higher than the experimental analysis. Analytical results showed 18% more amplification in the middle of the backfill for the dense state. The variation was found to be more than 34% at the top of the wall. About 21% difference between the analytical and experimental acceleration amplification was observed at the three-fourth height of the backfill. The above analysis found that for the lower density backfill, the variations were less than 7%. However, in the dense state, the variation was somehow higher (more than 18%). The dynamic properties used in the analytical model have been estimated from strain-controlled cyclic triaxial tests. The lower estimated shear modulus for dense sand might be contributing to the variation between analytical and experimental results.

CONCLUSION

This paper has summarised the results of an investigation of the influence of the wall inclination and different backfill density conditions on the seismic response of the geosynthetic reinforced soil walls. A series of 1-g shaking table tests were conducted by applying three different stepped amplitude sinusoidal base accelerations with incrementally increasing peak ground accelerations (PGA) amplitude. The major conclusions drawn from the experimental results are reported as follows:

- The input acceleration was found to amplify with the elevation of the wall and backfill having a nonlinear pattern. The AAF was increased by 30% at the top for 10^0 inward inclined wall compared to the vertical wall. The increase in pressure reduces damping and consequently increases amplification. With the increase in backfill density, AAF also increased. Dense soil exhibits lesser damping, which results in higher amplification. A vertical wall with dense sand backfills showed 13% greater AAF at top of the backfill than the loose state at high PGA.
- The middle of the wall experienced higher displacement, while the bottom wall experienced the least deformation. The wall deformation was found to reduce with the increase in wall inclination towards the backfill for the studied range of wall inclination. The lateral earth pressure decreases

with the increase in the inclination of the wall towards backfill as predicted in pseudo-static earth pressure theory. The 20^0 inward inclined wall showed 35.5% lesser displacement compared to the vertical wall at high PGA. In contrast, 10^0 outward inclined walls showed 16% higher deformation compared to the vertical wall due to unstable orientation.

- The dense backfill showed lower lateral displacement for both vertical and inclined walls. It was observed that wall deformation reduced by 21.5% at the middle of the wall for 10^0 inward inclined wall, however, the reduction in the vertical wall was marginal i.e., about 3% for high PGA. Dense backfill leads to more soil friction. The earth pressure coefficient decreases and thus wall deformation reduces.
- From the acceleration response and wall deformation measured for all the models, it can be concluded that the 20^0 inward inclined wall performed better compared to all other models. The horizontal displacement of the wall was minimum in this model. The AAF was also lower compared to that in other inward inclined wall models. Therefore, this inclination can be used in the MSE wall design for better performance.
- A simple analytical study was also used to calculate acceleration amplification in the soil backfill for the vertical MSE wall. The analytical results were compared with the experimental results of MSE walls with the loose and dense soil backfills. The analytical results showed the same pattern as that obtained from the experiment; however, the magnitude was higher in the analytical study. The analytical method used here does not consider soil-reinforcement interaction which may lead to higher amplification values.

Since soil behaviour is stress-dependent, the seismic response of these models may not truly reflect that of the prototype. Hence, the results from this study can only be used for understanding the effect of various dynamic shaking parameters on reinforced slopes but caution must be taken before extrapolating results for field-scale MSE walls.

List of Abbreviations:

MSE Mechanically stabilized earth
GRS Geosynthetic reinforced soil
PGA Peak ground acceleration
LVDT Linear variable differential transformer
FHWA Federal Highway Administration
H' Height of the wall
e_{max} Maximum void ratio
e_{min} Minimum void ratio
Rd Relative density
G Shear modulus
ω Circular frequency
H Soil thickness
ξ Damping coefficient
v_s Shear wave velocity
θ Wall inclination angle

Availability of data and material: Data will be made available on request.
Code availability: Not applicable

ACKNOWLEDGMENT

The Author (s) would like to greatly acknowledge to IIT Patna and the Department of Higher Education (Govt. of India) for providing the funding for the present research work for which no specific grant number has been allotted.

DECLARATIONS

Funding

Indian Institute of Technology Patna and Department of Higher Education (Govt. of India)

Conflicts of Interest/Competing Interests

The authors have no known competing financial interests or personal relationships that could have appeared to influence the work reported in this paper.

PROCESS DATES:

Received: August 29, 2021, Revision: June 16, 2022, Accepted: August 25, 2022

CORRESPONDING AUTHOR:

Correspondence should be addressed to Pradipta Chakrabortty; pradipt@gmail.com

REFERENCES

Abdelouhab, A., Dias, D., & Freitag, N. (2011). Numerical analysis of the behaviour of mechanically stabilized earth walls reinforced with different types of strips. *Geotextiles and Geomembranes*, *29*(2), 116–129. doi:10.1016/j.geotexmem.2010.10.011

Allen, T. M., & Bathurst, R. J. (2002). Soil reinforcement loads in geosynthetic walls at working stress conditions. *Geosynthetics International*, *9*(5-6), 525–566. doi:10.1680/gein.9.0227

ASTM. (2003). *Standard test methods for the determination of the modulus and damping properties of soils using the cyclic triaxial apparatus*. Author.

Bandyopadhyay, T. S., Chakrabortty, P., & Hegde, A. (2021). Shake Table Studies to Assess the Effect of Reinforced Backfill Parameters on Dynamic Response of MSE Walls. *Ground Improvement Techniques: Select Proceedings of 7th ICRAGEE 2020,* 227-237.

Bathurst, R. J. (2002). Shaking table model study on the dynamic response of reinforced soil walls. In *Proc. 7th Int. Geosynthetic Conf., Nice, France, 2002* (*Vol. 1*, pp. 99-102). Academic Press.

Bathurst, R. J., & Hatami, K. (1998). Seismic response analysis of a geosynthetic-reinforced soil retaining wall. *Geosynthetics International*, *5*(1-2), 127–166. doi:10.1680/gein.5.0117

Bathurst, R. J., Nernheim, A., Walters, D. L., Allen, T. M., Burgess, P., & Saunders, D. D. (2009). Influence of reinforcement stiffness and compaction on the performance of four geosynthetic-reinforced soil walls. *Geosynthetics International*, *16*(1), 43–59. doi:10.1680/gein.2009.16.1.43

Chen, H. T., Hung, W. Y., Chang, C. C., Chen, Y. J., & Lee, C. J. (2007). Centrifuge modeling test of a geotextile-reinforced wall with a very wet clayey backfill. *Geotextiles and Geomembranes*, *25*(6), 346–359. doi:10.1016/j.geotexmem.2007.01.003

Collin, J. G., Chouery-Curtis, V. E., & Berg, R. R. (1992). Field observations of reinforced soil structures under seismic loading. In *International symposium on earth reinforcement practice* (pp. 223-228). Academic Press.

El-Emam, M. M., & Bathurst, R. J. (2005). Facing contribution to seismic response of reduced-scale reinforced soil walls. *Geosynthetics International*, *12*(5), 215–238. doi:10.1680/gein.2005.12.5.215

El-Emam, M. M., & Bathurst, R. J. (2007). Influence of reinforcement parameters on the seismic response of reduced-scale reinforced soil retaining walls. *Geotextiles and Geomembranes*, *25*(1), 33–49. doi:10.1016/j.geotexmem.2006.09.001

Elias, V., Christopher, B. R., Berg, R. R., & Berg, R. R. (2001). *Mechanically stabilized earth walls and reinforced soil slopes: design and construction guidelines (updated version) (No. FHWA-NHI-00-043)*. United States Federal Highway Administration.

Huang, C. C., Horng, J. C., Chang, W. J., Chiou, J. S., & Chen, C. H. (2011). Dynamic behavior of reinforced walls–Horizontal displacement response. *Geotextiles and Geomembranes*, *29*(3), 257–267. doi:10.1016/j.geotexmem.2010.11.006

Huang, C. C., & Wang, W. C. (2005). Seismic displacement charts for the performance-based assessment of reinforced soil walls. *Geosynthetics International*, *12*(4), 176–190. doi:10.1680/gein.2005.12.4.176

Iai, S. (1989). Similitude for shaking table tests on soil-structure-fluid model in 1g gravitational field. *Soil and Foundation*, *29*(1), 105–118. doi:10.3208/sandf1972.29.105

Jackson, P., Bowman, E. T., & Cubrinovski, M. (2012). Seismic testing of model-scale geosynthetic-reinforced soil walls. *Bulletin of the New Zealand Society for Earthquake Engineering*, *45*(4), 171–183. doi:10.5459/bnzsee.45.4.171-183

Koseki, J. (2012). Use of geosynthetics to improve seismic performance of earth structures. *Geotextiles and Geomembranes*, *34*, 51–68. doi:10.1016/j.geotexmem.2012.03.001

Koseki, J., Munaf, Y., Sato, T., Tatsuoka, F., Tateyama, M., & Kojima, K. (1998). Shaking and tilt table tests of geosynthetic-reinforced soil and conventional-type retaining walls. *Geosynthetics International*, *5*(1-2), 73–96. doi:10.1680/gein.5.0115

Kramer, S. L. (1996). *Geotechnical earthquake engineering*. Pearson Education India.

Latha, G. M., & Krishna, A. M. (2008). Seismic response of reinforced soil retaining wall models: Influence of backfill relative density. *Geotextiles and Geomembranes*, *26*(4), 335–349. doi:10.1016/j.geotexmem.2007.11.001

Latha, G. M., & Santhanakumar, P. (2015). Seismic response of reduced-scale modular block and rigid faced reinforced walls through shaking table tests. *Geotextiles and Geomembranes*, *43*(4), 307–316. doi:10.1016/j.geotexmem.2015.04.008

Latha, G. M., & Somwanshi, A. (2009). Bearing capacity of square footings on geosynthetic reinforced sand. *Geotextiles and Geomembranes*, *27*(4), 281–294.

Lee, K. L., Adams, B. D., & Vagneron, J. M. J. (1973). Reinforced earth retaining walls. *Journal of the Soil Mechanics and Foundations Division*, *99*(10), 745–764. doi:10.1061/JSFEAQ.0001931

Lemnitzer, A., Hilson, C., Nojoumi, A., Taciroglu, E., Wallace, J. W., & Stewart, J. P. (2012). Experimental Assessment of the Passive Resistance of a Bridge Abutment System with Various Backfill Heights. In *GeoCongress 2012* (pp. 2088–2097). State of the Art and Practice in Geotechnical Engineering. doi:10.1061/9780784412121.214

Ling, H. I., Mohri, Y., Leshchinsky, D., Burke, C., Matsushima, K., & Liu, H. (2005). Large-scale shaking table tests on modular-block reinforced soil retaining walls. *Journal of Geotechnical and Geoenvironmental Engineering*, *131*(4), 465–476. doi:10.1061/(ASCE)1090-0241(2005)131:4(465)

Ling, H. I., Yang, S., Leshchinsky, D., Liu, H., & Burke, C. (2010). Finite-element simulations of full-scale modular-block reinforced soil retaining walls under earthquake loading. *Journal of Engineering Mechanics*, *136*(5), 653–661. doi:10.1061/(ASCE)EM.1943-7889.0000108

Liu, H., Yang, G., & Ling, H. I. (2014). Seismic response of multi-tiered reinforced soil retaining walls. *Soil Dynamics and Earthquake Engineering*, *61*, 1–12. doi:10.1016/j.soildyn.2014.01.012

Matsuo, O., Yokoyama, K., & Saito, Y. (1998). Shaking table tests and analyses of geosynthetic-reinforced soil retaining walls. *Geosynthetics International*, *5*(1-2), 97–126. doi:10.1680/gein.5.0116

Murata, O. (1994). Shaking table tests on a large geosynthetic-reinforced soil retaining wall model. *Recent case histories of permanent geosynthetic-reinforced soil retaining walls, 1*, 259-264.

Nandan, S. K., Bandyopadhyay, T. S., & Chakrabortty, P. (2021). Effect of Backfill Sand Density on Dynamic Response of Mechanically Stabilized Earth (MSE) Walls. *Proceedings of the Indian Geotechnical Conference 2019,* 817-827.

Pamuk, A., Ling, H. I., Leshchinsky, D., Kalkan, E., & Adalier, K. (2004). Behavior of reinforced wall system during the 1999 Kocaeli (Izmit), Turkey earthquake. In *Proceedings of the 5th International Conference on Case Histories in Geotechnical Engineering* (pp. 13-17). Academic Press.

Riccio, M., Mauricio, E., & Daniel, D. (2014). Field monitoring and analyses of the response of a block-faced geogrid wall using fine-grained tropical soils. *Geotextiles and Geomembranes*, *42*(2), 127–138. doi:10.1016/j.geotexmem.2014.01.006

Sakaguchi, M. (1996). A study of the seismic behavior of geosynthetic reinforced walls in Japan. *Geosynthetics International*, *3*(1), 13–30. doi:10.1680/gein.3.0051

Srilatha, N., Latha, G. M., & Puttappa, C. G. (2016). Seismic response of soil slopes in shaking table tests: Effect of type and quantity of reinforcement. *International Journal of Geosynthetics and Ground Engineering*, *2*(4), 1–13. doi:10.1007/s40891-016-0074-2

Tatsuoka, F. (1993). Roles of facing rigidity in soil reinforcing. In *International symposium on earth reinforcement practice* (pp. 831-870). Academic Press.

Tatsuoka, F., Tateyama, M., & Koseki, J. (1996). Performance of soil retaining walls for railway embankments. *Soil and Foundation*, *36*(Special), 311–324. doi:10.3208/sandf.36.Special_311

Tatsuoka, F., Tateyama, M., Uchimura, T., & Koseki, J. (1997). Geosynthetic-reinforced soil retaining walls as important permanent structures 1996-1997 mercer lecture. *Geosynthetics International*, *4*(2), 81–136. doi:10.1680/gein.4.0090

Wang, L., Chen, G., & Chen, S. (2015). Experimental study on seismic response of geogrid reinforced rigid retaining walls with saturated backfill sand. *Geotextiles and Geomembranes*, *43*(1), 35–45. doi:10.1016/j.geotexmem.2014.11.006

Yang, G., Liu, H., Lv, P., & Zhang, B. (2012). Geogrid-reinforced lime-treated cohesive soil retaining wall: Case study and implications. *Geotextiles and Geomembranes*, *35*, 112–118. doi:10.1016/j.geotexmem.2012.09.001

Yang, G., Zhang, B., Lv, P., & Zhou, Q. (2009). Behaviour of geogrid reinforced soil retaining wall with concrete-rigid facing. *Geotextiles and Geomembranes*, *27*(5), 350–356. doi:10.1016/j.geotexmem.2009.03.001

Yang, K. H., Hung, W. Y., & Kencana, E. Y. (2013). Acceleration-amplified responses of geosynthetic-reinforced soil structures with a wide range of input ground accelerations. In Geo-Congress 2013: Stability and Performance of Slopes and Embankments III (pp. 1178-1187). Academic Press.

Zhang, F., Leshchinsky, D., Gao, Y., & Leshchinsky, B. (2014). Required unfactored strength of geosynthetics in reinforced 3D slopes. *Geotextiles and Geomembranes*, *42*(6), 576–585. doi:10.1016/j.geotexmem.2014.10.006

Tirtha Sathi Bandyopadhyay is a research scholar in the Department of Civil and Environmental Engineering at Indian Institute of Technology Patna, India. He obtained his MTech degree in Soil and Foundation Engineering from Birsa Institute of Technology Sindri, India in 2016. He graduated from Chhattisgarh Swami Vivekanand Technical University Bhilai, India in the field of civil engineering in the year 2014. His research interests include ground improvement and geosynthetics, stability of earth retaining structures, geotechnical earthquake engineering.

Sumit Kumar Nandan completed B.Tech in Civil Engineering from IIT Patna in 2019. My research area of interest is Mechanically Stabilized Earth Wall (MSE Wall).

Pradipta Chakrabortty is Assistant Professor of geotechnical engineering, at the Department of Civil and Environmental Engineering, Indian Institute of Technology Patna (IITP) India. He specializes in soil dynamics, geotechnical earthquake engineering, site characterization, microzonation, dynamic soil-structure interaction, and low-cost housing. His research has been mainly sponsored by Department of Science and Technology (DST) New Delhi, and Ministry of Human Resources of Government of India. He has authored and co-authored over 50 scientific papers in journals and conferences and has served as reviewer for over 10 Journals. He received the B.E. degree in Civil Engineering from Jadavpur University, Kolkata, India, in 2000; the M. Tech. degree in Earthquake Engineering from Indian Institute of Technology Roorkee, India, in 2002 and the Ph.D. degree in Civil Engineering from Memorial University of Newfoundland, St. John's, Canada, in 2009. In 2009 he worked in a central government PSU, National Building Construction Corporation (India) Ltd. From 2009 to 2012, he was with Civil Engineering department of Birla Institute of Technology and Science, Pilani Campus, India. He has received the Indian Service of Engineers award for his performance during M. Tech. He was a recipient of Fellow of the school of graduate studies award in 2009 from Memorial University of Newfoundland for his outstanding achievement and contribution during PhD.